HHS Public Access

Author manuscript

Eur J Radiol. Author manuscript; available in PMC 2022 June 01.

Published in final edited form as:

Eur J Radiol. 2021 June ; 139: 109679. doi:10.1016/j.ejrad.2021.109679.

Cine MRI characterizes HFpEF and HFrEF in post-capillary pulmonary hypertension

Kai Lin, MD, MS, **Roberto Sarnari, MD**, **Ashitha Pathrose, MD**, **Daniel Z. Gordon, PhD**, **Julie Blaisdell, MS**, **Michael Markl, PhD**, **James C. Carr, MD**

Department of Radiology, Northwestern University, 737 N Michigan Avenue, Suite 1600, Chicago, IL 60611

Abstract

Purpose—To test the hypothesis that cine MRI can be used to characterize features of left and right ventricles in post-capillary pulmonary hypertension (PH) caused by heart failure (HF) with preserved ejection fraction (HFpEF) and HF with reduced ejection fraction (HFrEF).

Methods—With the approval of institution review board (IRB), 28 consecutive post-capillary PH patients (11 males, 62.1 ± 13.4 years old, range 39 –89 years old) underwent cine MRI scans. Cine MRI-derived left ventricular (LV) ejection fraction (LVEF) and other function, motion, and deformation indices (acquired with heart deformation analysis [HDA]) were compared between PH-HFpEF (defined as LVEF ≥ 50%]) and PH-HFrEF (LVEF < 50%) patients and were related with right ventricular (RV) indices and right heart catheterization (RHC)-derived pulmonary artery measurements.

Results—Totally 19 patients (68%, 95% confident interval [CI] 49% - 86%) were assigned to PH-HFpEF group while 9 (32%) was assigned to the PH-HFrEF group. There were differences of LV and right ventricular (RV) global functional indices, LV mass, LV displacement, velocity, strain and strain rate between the two patient groups. Cine MRI-derived LV indices had broad associations with RV indices and RHC measurements. LVEF was negatively correlated with pulmonary capillary wedge pressure (PCWP) ($r = -0.5$, $p = 0.007$). LV cardiac index (LVCI) was associated with systolic pulmonary artery pressure (sPAP) ($r = 0.443$, $p = 0.018$).

Conclusions—PH-HFpEF and PH-HFrEF patients present dissimilar function, motion and deformation features in LV and RV. Cine MRI-derived LV measures are correlated with hemodynamic abnormalities of PH.

Address for correspondence: Kai Lin (kai-lin@northwestern.edu), Department of Radiology, Northwestern University, 737 N Michigan Avenue, Suite 1600, Chicago, IL 60611, Tel: (312)695-5577, Fax: (312)926-5991.

CRediT authorship contribution statement

Kai Lin: Conceptualization, Methodology, Writing- Original draft preparation

Roberto Sarnari, Ashitha Pathrose, Daniel Gordon, Julie Blaisdell: data curation

Michael Markl, James Carr: Conceptualization, Supervision

Keywords

Cine MRI; post-capillary pulmonary hypertension; HFpEF; HFrEF; heart deformation analysis

Introduction

Post-capillary pulmonary hypertension (PH) is a common type of PH resulting from an elevated left heart pressure [1]. Heart failure (HF), which usually represents irreversible left ventricular (LV) damages after advanced cardiovascular diseases (CVDs), serves as a major cause of post-capillary PH. HF is a highly heterogeneous pathological condition and its clinical manifestations are diverse. HF can be simply divided into two types, the HF with preserved ejection fraction (HFpEF) and HF with reduced ejection fraction (HFrEF), according to the levels of LV ejection fraction (LVEF). Manifestations of PH originating from HFpEF and HFrEF can be different because these two types of HF have disparate pathophysiological mechanisms and hemodynamic changes [2]. Therefore, characterization of PH-HFpEF and PH-HFrEF related functional and structural abnormalities can be important in PH management because the information is expected to reflect the severity and progression of PH and can be used to guide targeted therapies.

Cine magnetic resonance imaging (MRI) provides good contrast between the myocardium and the blood pool for dynamically describing contraction and relaxation of the heart during a cardiac cycle [3, 4]. To date, cine MRI has become a well-accepted imaging modality for the evaluation of global LV and right ventricular (RV) function. In addition, information regarding global and regional LV motion/deformation patterns can also be automatically extracted from regular cine MRI datasets using advanced image processing techniques, such as heart deformation analysis (HDA) [5–8], In the present study, we acquired cine MRI-derived LV and RV function, motion and deformation indices of 28 post-capillary PH patients who were diagnosed with right heart catheterization (RHC). The aim of the present study was to test the hypothesis that cine MRI can be used to characterize features of LV and RV in post-capillary PH caused by HFpEF and HFrEF.

Materials and methods

Patient population

With the approval of institution review board (IRB), 28 consecutive post-capillary PH patients (11 males, 60.1 ± 13.5 years old, range 39 –89 years old) underwent a cardiac MRI scan. All patients were diagnosed the RHC. Post-capillary PH was defined as mean pulmonary arterial pressure (mPAP) ⩾ 25 mmHg and pulmonary capillary wedge pressure (PCWP)> 15 mmHg [9], Post-capillary PH with a pulmonary vascular resistance (PVR) > 3 wood units were marked as having a “reactive PH” [10], All participants provided written informed consents before the MRI scan.

Inclusion criteria: 1) age 18 - 89 years; 2) male or female with clinically diagnosed PH Exclusion criteria: 1) with valvar diseases, congenital heart diseases or pericardial constriction; 2) presence of a permanent pacemaker or cardioverter-defibrillator; 3) prior

stroke, neurodegenerative disorders, mental health problems or malignances; 4) chronic or acute kidney disease (eGFR < 30mL/min/1.73m^2); and 5) any other contraindications to MRI, such as implanted metal device or claustrophobia.

Cine MRI protocol

Cardiac MRI examinations were performed on a 1.5 T scanner (Magnetom, Aera, SIEMENS, Erlangen, Germany) using a fixed protocol. A three-plane fast localization sequence was applied to find anatomic orientation of the entire scan. Then, a segmented balanced steady-state free precession (bSSFP) pulse sequence was employed in the 2, 3, 4-chamber and short-axis orientations to acquire cine images. Imaging parameters were as follows: Repetition time (TR)/Echo time (TE) = 35.5/1.2 ms; flip angle = 80°; slice thickness = 6 mm; gap = 4 mm; base resolution = 192; bandwidth = 930 Hz/pixel; with generalized autocalibrating partially parallel acquisition (GRAPPA) technique and reduction factor R = 2. Each myocardial slice was acquired during a breath-hold at end-expiration using retrospective electrocardiogram (ECG) gating (with 25 retrospectively constructed cardiac phases). Ten to twelve short-axis slices were acquired to cover the entire LV from base to apex [11].

Regular processes on cine MRI datasets

Cine images were processed on the dedicated workstation affiliated to the MRI scanner by an experience operator (_, 5 years of experience in cardiovascular radiology) using Argus (Siemens, Erlangen, Germany). For each slice and time phase, the epicardial and endocardial borders of LV and RV were carefully traced manually. LV and RV volumes at each cardiac phase were obtained by summing the LV areas of all slices from the base to the apex of the ventricles. The end-diastolic volume (LVEDV and RVEDV), end-systolic volume (LVESV and RVESV), stroke volume (LVSV and RVSV), cardiac output (LVCO and RVCO), cardiac index (LVCI and RVCI), ejection fraction (LVEF and RVEF) and LV mass (LVM) were then calculated.

HDA analysis on cine MRI datasets

All de-identified cine images were transferred to a dedicated image processing workstation (HP, EliteDesk 800 G2 TWR)and analyzed with a prototype software of HDA programmed in Visual C++ (TrufiStrain, version 2.0, Siemens, Erlangen, Germany) by another analyzer (_,with 17 years of experience in cardiovascular imaging). The HDA automatically detected cardiac landmarks and defined epicardial and endocardial myocardial borders based on an algorithm that was previously described [12], Using an existing deformation inversion recovery (DIR) algorithm, HDA could automatically calculate frame-to-frame motion deformation fields on cine images [13], Between any two cardiac time frames for a given transversal LV plane, a dense deformation was computed using gradient descent minimization. At every step of the gradient descent minimization, the image registration remained inversely consistent by solving for the deformation fields and the inverse deformation fields. Global and segmental myocardial motion indices, including displacement (defined as the shortest distance from the initial to the final position), velocity (displacement/time), strain ([change in length]/[original length]), and strain rate (change of stain/time), were derived from the variant deformation fields over time. Next, in-plane time-

resolved regional myocardial motion vectors in the radial and circumferential directions were calculated for the entire LV (global values) for each patient. Peak values of each LV motion/deformation indices were acquired from time curves though the entire cardiac cycle using an existing method [11, 14].

RHC

As a part of the “standard of care”, patients were examined with cardiologists in our institution. In the supine position, standard RHC was performed through a 7–9 F sheath via the internal jugular or femoral vein. Swan-Ganz catheter was then inserted. Systolic, diastolic and mean pulmonary artery pressure (sPAP, dPAP, mPAP) and PCWP were measured at end-expiration from continuous recordings of pressure tracings digitized at 240 Hz and represent the mean of ⩾3 beats. PVR was then calculated as (mPAP-PCWP)/LVCO.

Data processing and statistical methods

Data were expressed as the mean ± standard deviation (SD). PH patients were divided into PH-HFpEF and PH-HFrEF groups base on LVEF (≥ 50% vs. < 50%). Demographic and clinical data of PH, global peak myocardial motion/deformation indices (along radial and circumferential directions) in early and late diastole were extracted and compared between two patient groups using t-tests, Chi-square tests or Fisher’s exact test. Cine MRI-derived LV indices were related with RV indices and RHC measurements using Pearson correlation coefficient (r).

Statistical analysis was performed by using SPSS software (Version 22, IBM Corporation). A p value < 0.05 was considered statistically significant.

Results

Cine MRI were completed in 28 post-capillary PH patients. All cine images were eligible for quantitative analysis. The mean interval between MRI and RHC was 20.9 ± 6.6 days.

Totally 19 patients (68%, 95% confident interval [CI] 49% -86%) was assigned to PH-HFpEF group while 9 (32%) was assigned to the PH-HFrEF group. There were no differences on demographic data or the prevalence of reactive PH between two patient groups.

Compared to PH-HFrEF patients, PH-HFpEF patients had lower LVM (98.8 ±21.8 g vs. 125.9± 24.2 g, p = 0.006), LVEDV (143.5 ± 57.5 mL vs. 193.4 ± 59.1 mL, p = 0.043), LVESV (54.6 ± 30.3 mL vs. 127.1 ± 48.6 mL, p < 0.001) and higher LVCI (2.88 ± 0.88 L/min/m^2 vs. 2.16 ± 0.56 L/min/m^2, p = 0.033), RVSV (84.1 ± 23.5 mL vs. 62.5 ± 25.3 mL, p = 0.035), RVCO (5.64 ± 1.81 L/min vs. 4.14 ± 1.29 L/min, p = 0.036) and RVCI (2.75 ± 0.9 L/min/m^2 vs. 2.02 ± 0.67 L/min/m^2, p = 0.041). See table 1. PH-HFpEF patients had higher peak radial displacement, velocity, strain and strain rates in systole and diastole than that of PH-HFrEF patients. See table 2. Figure 1 showed comparisons of radial and circumferential strain rates between cases of PH-HFpEF and PH-HFrEF.

LV function indices were related with RV function indices and RHC measures. LVEF had significant correlations with PCWP (r = −0.5, p = 0.007), RVSV (r = 0.477, p = 0.01), RVCO (r = 0.442, p = 0.019) and RVCI (r= 0.453, p = 0.015). LVESV was associated with PCWP (r = 0.488, p = 0.008). LVSV was linked to RVEDV (r = 0.548, p = 0.003), RVSV (0.53, p = 0.004) and RVCO (r = 0.454, p = 0.015). LVCO was associated with RVEDV (r = 0.636, p < 0.001), RVESV (r = 0.464, p = 0.013), RVSV (r = 0.413, p = 0.029) and RVCO (r = 0.51, p = 0.006), LVCI was correlated with sPAP (r = 0.443, p = 0.018), RVEDV (r = 0.538, p = 0.003), RVSV (r = 0.454, p = 0.015), RVCO (r = 0.542, p = 0.003), and RVCI (r = 0.592, p = 0.001). See figure 2.

LV motion and deformation indices were also related with RV function. Peak systolic radial displacement (r = 0.428, p = 0.023) and velocity (r = 0.441, p = 0.015) were related with RVSV. Peak early radial diastolic velocity was associated with RVEDV (r = 0.448, p = 0.017). Peak radial strain was related with RVSV (r = 0.625, p < 0.001), RVCO (r = 0.459, p = 0.014), RVEF (r = 0.496, p = 0.007) and RVCI (r = 0.491, p = 0.008). Peak circumferential strain was related with RVSV (r = 0.498, p = 0.007). Peak radial systolic strain rate was related with RVSV (r = 0.511, p = 0.005), RVCO (r = 0.455, p = 0.015), and RVCI (r = 0.466, p = 0.012).

Discussion

Based on regular cine MRI and HDA processing, we characterized LV and RV function, LV motion and deformation patterns in post-capillary PH caused by HFpEF and HFrEF. Structural and functional similarities and differences between PH-HFpEF and PH-HFrEF were described in the LV and RV. Multiple LV indices were shown to have correlations with MRI-derived RV functional indices and homodynamic parameters measured by RHC. Our results showed that that cine MRI is able to provide rich and detailed information regarding clinical manifestations of HFpEF and HFrEF in the context of PH.

Both HFpEF and HFrEF can result in post-capillary PH [2]. Generally, the incidence of HFpEF is associated with female, older age, and systemic disorders that intend to result in systemic changes in cardiovascular microenviroments, such as metabolic syndromes [15]. While HFrEF is usually more common in younger population with structural CVDs, such as coronary heart disease (CHD) or dilated cardiomyopathy (DCM) [16]. Generally, HFpEF was thought to be driven by an impaired LV diastolic function while HFrEF was due to an impaired LV systolic function. Our data showed that PH-HFrEF patients seemed to suffer more severe myocardial incapability in both systole and diastole as compared with PH-HFpEF patients demonstrated by widely lower magnitudes of LV displacement, velocity, strain and strain rates. PH-HFrEF patients also had a much higher LVM than PH-HFpEF patients. At the same time, RV performance in PH-HFrEF was also lower than that in PH-HFpEF.

Representing changes of both the preload and afterload of the LV, LVEF is the traditional measurement of LV performance for discriminating HFpEF from HFrEF. However, there is still controversy on the prognosis estimation for HF based on the level of LVEF. Despite the different levels of LVEF, HFpEF and FIFrEF patients seemed to have similar mortality rates.

Shah et al constructed multivariable models to investigate clinical outcomes of 39,982 hospitalized HF patients from 254 hospitals who were admitted between 2005 and 2009. There was no difference between 5-year mortality rates of 18,398 HFrEF (75.7%) and 18,299 HFpEF (75.3%) patients (hazard ratio [HR]: 0.99, 95% CI: 0.958 to 1.022) [17], However, Curtis et al followed 7,788 outpatients with stable HF for 37 months. The authors found that the mortality of those patients with a baseline LVEF < 45% was linearly related with the level of LVEF after the adjustments of multiple cardiovascular risk factors. In patients with LVEF < 15%, the mortality was 51.7% while in patients with LVEF between 36% to 45%, the mortality lowered to 25.6% ($p < 0.0001$) [18], Ghimire et al followed HFrEF patients with repeated echocardiograms. Compared to those with persistent HFrEF, those HFrEF patients with > 10% increase in LVEF had a significant lower rate of adverse clinical events, including death, hospitalization, and heart transplantation [19], From a different aspect, the present study examined HFpEF and HFrEF in the context of PH, a clinical manifestation that usually suggests an adverse prognosis of HF patients [20], Our results demonstrated that a decreased LVEF was associated with an increased PCWP, an independent predictor of clinical outcomes of HFpEF [21], Additionally, LVCI, an index reflecting normalized LV pumping performance was related to an elevated sPAP. Our findings suggested that cine MRI-derived measures may have the potential to provide new insight into the prognosis estimation for HF and PH patients.

It is worth noted that “reactive PH”, also known as “combined pre- and post-capillary PH (cpc-PH)”, is a special subgroup of PH usually rising from some post-capillary PH cases. Induced by a long-term elevated PCWP, pulmonary vascular wall can be remodeled and result in a pathological change that is similar to that of idiopathic pulmonary artery hypertension (iPAH) [22], Contributed by disorders in both systemic and pulmonary circulations, reactive PH usually presents a “disproportionally” high mPAP, a high transpulmonary pressure gradient (TPG) and PVR. Previous studies showed that cpc-PH could be found in around 12%-14% patients receiving RHC examinations [23], However, the prevalence of reactive PH in PH-HFpEF and PH-HFrEF had not been reported separately. Our data demonstrated that a large portion of PH-HFpEF and PH-HFrEF patients having reactive PH. However, there seemed to be no significant differences on the levels of PVR or the prevalence of reactive PH between PH-HFpEF and PH-HFrEF patients.

Our study had limitations. First, the sample size was small due to availability of stable PH patients. As a result, we were unable to balance all traditional cardiovascular risk conditions during the comparisons. Second, limited by the design of the original study, the clinical outcomes of those post-PH patients were not available. Therefore, we were unable to estimate the value of MRI-derived cardiac function, motion and deformation indices for predicting prognosis of post-capillary PH patients. Third, limited by current HDA software, the RV and left atrial (LA) motion/deformation indices could not be extracted from regular cine MRI datasets automatically. Therefore, those indices were not included in the present study.

In conclusion, PH-HFpEF and PH-HFrEF patients present dissimilar function, motion and deformation features in LV and RV. Cine MRI-derived LV measures are correlated with hemodynamic abnormalities of PH.

Conflict of interest

This study was partly supported by grants from the National Institute of Health (K01HL121162 and R03HL144891 to KL).

This study was supported by a grant from Bayer Pharmaceutical. The grant was paid to the institution not to individual researchers. James C. Carr has disclosure: Siemens: research grant to institution; advisory board. Bayer: research grant to institution; advisory board; speaker. Bracco: advisory board. Guerbet: research grant to institution. Other authors have nothing to disclose.

This study was partly supported by grants from the National Institute of Health (K01HL121162 and R03HL144891 to KL).

This study was supported by a grant from Bayer Pharmaceutical. The grant was paid to the institution not to individual researchers. James C. Carr has disclosure: Siemens: research grant to institution; advisory board. Bayer: research grant to institution; advisory board; speaker. Bracco: advisory board. Guerbet: research grant to institution. Other authors have nothing to disclose.

References

[1]. Naeije R, Chin K, Differentiating Precapillary From Postcapillary Pulmonary Hypertension, Circulation 140(9) (2019) 712–714. [PubMed: 31449453]

[2]. Guazzi M, Ghio S, Adir Y, Pulmonary Hypertension in HFpEF and HFrEF: JACC Review Topic of the Week, Journal of the American College of Cardiology 76(9) (2020) 1102–1111. [PubMed: 32854845]

[3]. Malayeri AA, Johnson WC, Macedo R, Bathon J, Lima JA, Bluemke DA, Cardiac cine MRI: Quantification of the relationship between fast gradient echo and steady-state free precession for determination of myocardial mass and volumes, J Magn Reson Imaging 28(1) (2008) 60–6. [PubMed: 18581356]

[4]. Khan MA, Yang EY, Zhan Y, Judd RM, Chan W, Nabi F, Heitner JF, Kim RJ, Klem I, Nagueh SF, Shah DJ, Association of left atrial volume index and all-cause mortality in patients referred for routine cardiovascular magnetic resonance: a multicenter study, J Cardiovasc Magn Reson 21(1) (2019) 4.

[5]. Lin K, Collins JD, Chowdhary V, Markl M, Carr JC, Heart deformation analysis for automated quantification of cardiac function and regional myocardial motion patterns: A proof of concept study in patients with cardiomyopathy and healthy subjects, European journal of radiology 85(10) (2016) 1811–1817. [PubMed: 27666621]

[6]. Lin K, Collins JD, Chowdhary V, Markl M, Carr JC, Heart deformation analysis: measuring regional myocardial velocity with MR imaging, The international journal of cardiovascular imaging 32(7) (2016) 1103–11. [PubMed: 27076222]

[7]. Lin K, Collins JD, Lloyd-Jones DM, Jolly MP, Li D, Markl M, Carr JC, Automated Assessment of Left Ventricular Function and Mass Using Heart Deformation Analysis:: Initial Experience in 160 Older Adults, Academic radiology (2015).

[8]. Meng L, Lin K, Collins J, Markl M, Carr JC, Automated Description of Regional Left Ventricular Motion in Patients With Cardiac Amyloidosis: A Quantitative Study Using Heart Deformation Analysis, AJR. American journal of roentgenology 209(2) (2017) W57–W63. [PubMed: 28537770]

[9]. Rosenkranz S, Preston IR, Right heart catheterisation: best practice and pitfalls in pulmonary hypertension, European respiratory review : an official journal of the European Respiratory Society 24(138) (2015) 642–52. [PubMed: 26621978]

[10]. Aronson D, Eitan A, Dragu R, Burger AJ, Relationship between reactive pulmonary hypertension and mortality in patients with acute decompensated heart failure, Circulation. Heart failure 4(5) (2011) 644–50. [PubMed: 21606213]

[11]. Lin K, Sarnari R, Pathrose A, Gordon D, Blaisdell J, Markl M, Carr JC, Cine MRI detects elevated left heart pressure in pulmonary hypertension, Journal of magnetic resonance imaging : JMRI (2021).

[12]. Jolly M-P, Guetter C, Lu X, Xue H, Guehring J, Automatic Segmentation of the Myocardium in Cine MR Images Using Deformable Registration, Statistical Atlases and Computational Models of the Heart. Imaging and Modelling Challenges 7085 (2012) 98–108.

[13]. Guetter CX, Chefd'hotel H, Guehring C, J., Efficient symmetric and inverse-consistent deformable registration through interleaved optimization, Biomedical Imaging: From Nano to Macro, 2011 IEEE International Symposium on, 2011, p. 4.

[14]. Lin K, Ma H, Sarnari R, Li D, Lloyd-Jones DM, Markl M, Carr JC, Cardiac MRI Reveals Late Diastolic Changes in Left Ventricular Relaxation Patterns During Healthy Aging, Journal of magnetic resonance imaging : JMRI 53(3) (2021) 766–774. [PubMed: 33006438]

[15]. Shah SJ, Borlaug BA, Kitzman DW, McCulloch AD, Blaxall BC, Agarwal R, Chirinos JA, Collins S, Deo RC, Gladwin MT, Granzier H, Hummel SL, Kass DA, Redfield MM, Sam F, Wang TJ, Desvigne-Nickens P, Adhikari BB, Research Priorities for Heart Failure With Preserved Ejection Fraction: National Heart, Lung, and Blood Institute Working Group Summary, Circulation 141(12) (2020) 1001–1026. [PubMed: 32202936]

[16]. Gopal DM, Santhanakrishnan R, Wang YC, Ayalon N, Donohue C, Rahban Y, Perez AJ, Downing J, Liang CS, Gokce N, Colucci WS, Ho JE, Impaired right ventricular hemodynamics indicate preclinical pulmonary hypertension in patients with metabolic syndrome, Journal of the American Heart Association 4(3) (2015) e001597. [PubMed: 25758604]

[17]. Shah KS, Xu H, Matsouaka RA, Bhatt DL, Heidenreich PA, Hernandez AF, Devore AD, Yancy CW, Fonarow GC, Heart Failure With Preserved, Borderline, and Reduced Ejection Fraction: 5-Year Outcomes, Journal of the American College of Cardiology 70(20) (2017) 2476–2486. [PubMed: 29141781]

[18]. Curtis JP, Sokol SI, Wang Y, Rathore SS, Ko DT, Jadbabaie F, Portnay EL, Marshalko SJ, Radford MJ, Krumholz HM, The association of left ventricular ejection fraction, mortality, and cause of death in stable outpatients with heart failure, Journal of the American College of Cardiology 42(4) (2003) 736–42. [PubMed: 12932612]

[19]. Ghimire A, Fine N, Ezekowitz JA, Howlett J, Youngson E, McAlister FA, Frequency, predictors, and prognosis of ejection fraction improvement in heart failure: an echocardiogram-based registry study, European heart journal 40(26) (2019) 2110–2117. [PubMed: 31280320]

[20]. Chatterjee NA, Lewis GD, What is the prognostic significance of pulmonary hypertension in heart failure?, Circulation. Heart failure 4(5) (2011) 541–5. [PubMed: 21934090]

[21]. Dorfs S, Zeh W, Hochholzer W, Jander N, Kienzle RP, Pieske B, Neumann FJ, Pulmonary capillary wedge pressure during exercise and long-term mortality in patients with suspected heart failure with preserved ejection fraction, European heart journal 35(44) (2014) 3103–12. [PubMed: 25161181]

[22]. Rao SD, Adusumalli S, Mazurek JA, Pulmonary Hypertension in Heart Failure Patients, Cardiac failure review 6 (2020) e05. [PubMed: 32377384]

[23]. Naeije R, Gerges M, Vachiery JL, Caravita S, Gerges C, Lang IM, Hemodynamic Phenotyping of Pulmonary Hypertension in Left Heart Failure, Circulation. Heart failure 10(9) (2017).

Highlights

- In patients with post-capillary pulmonary hypertension (PH), cine MRI-derived left ventricular (LV) function, motion, deformation indices have broad relations with right ventricular (RV) indices and right heart catheterization (RHC) measurements.
- There are significant differences on the levels of multiple LV and RV indices between post-capillary PH caused by HFpEF and HFrEF.
- There is no difference on the incidence of reactive PH in post-capillary PH caused by HFpEF and HFrEF.

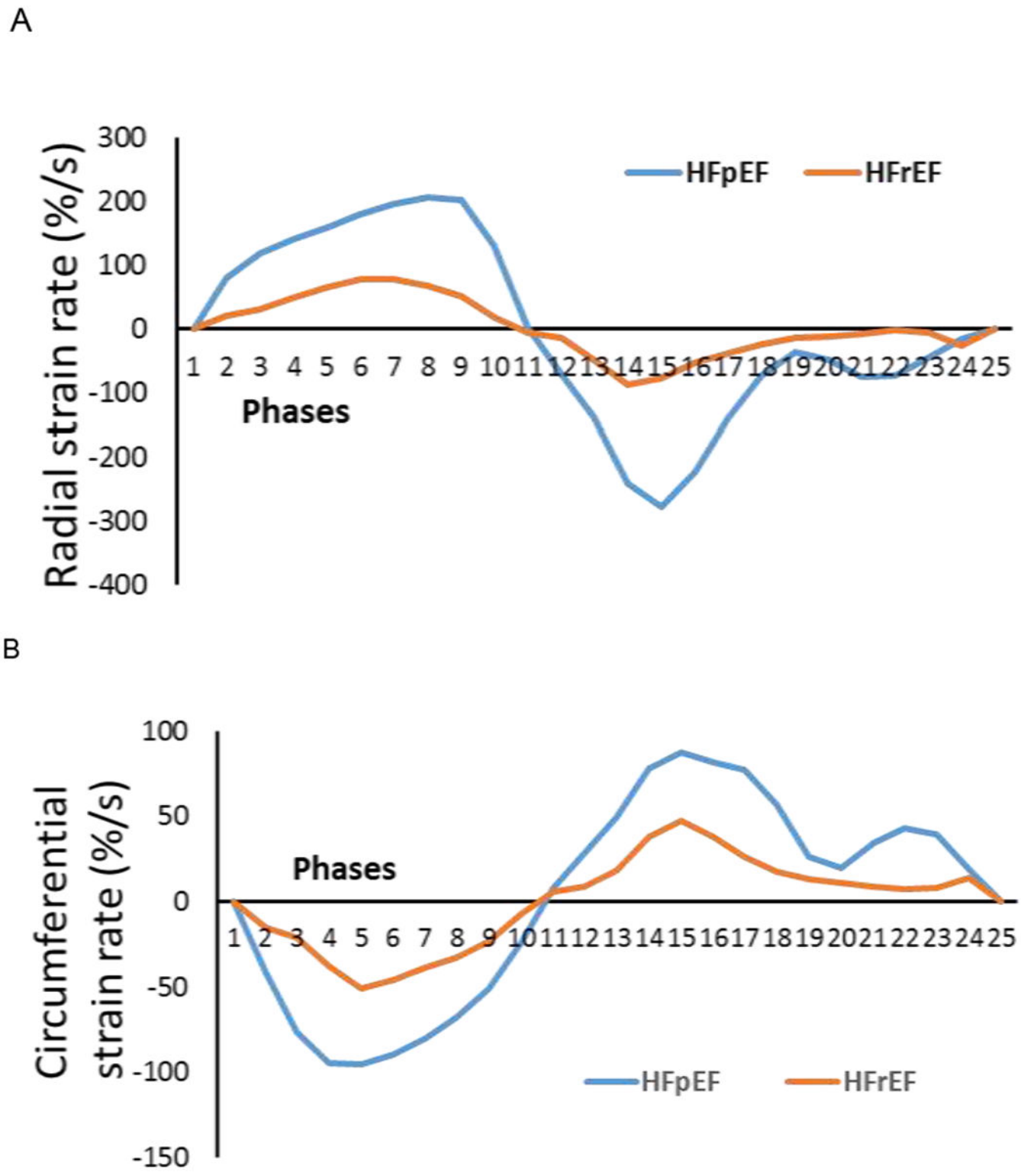

Figure 1.

Time curves through a cardiac cycle (25 phases from cine images) showed that a PH-HFpEF patient (female, 58 years old, LVEF = 70%, mPAP = 47 mmHg, PCWP = 20 mmHg, PVR =

3.32 wood units) had high peak values in systole (phases 1 – 11), early (phases 12 – 18) and late diastole (phases 19 – 25) than a PH-HFrEF patient (female, 73 years old, LVEF =35%, mPAP = 35 mmHg, PCWP = 23 mmHg, PVR = 3.46 wood units) in radial (A) and circumferential (B) strain rates.

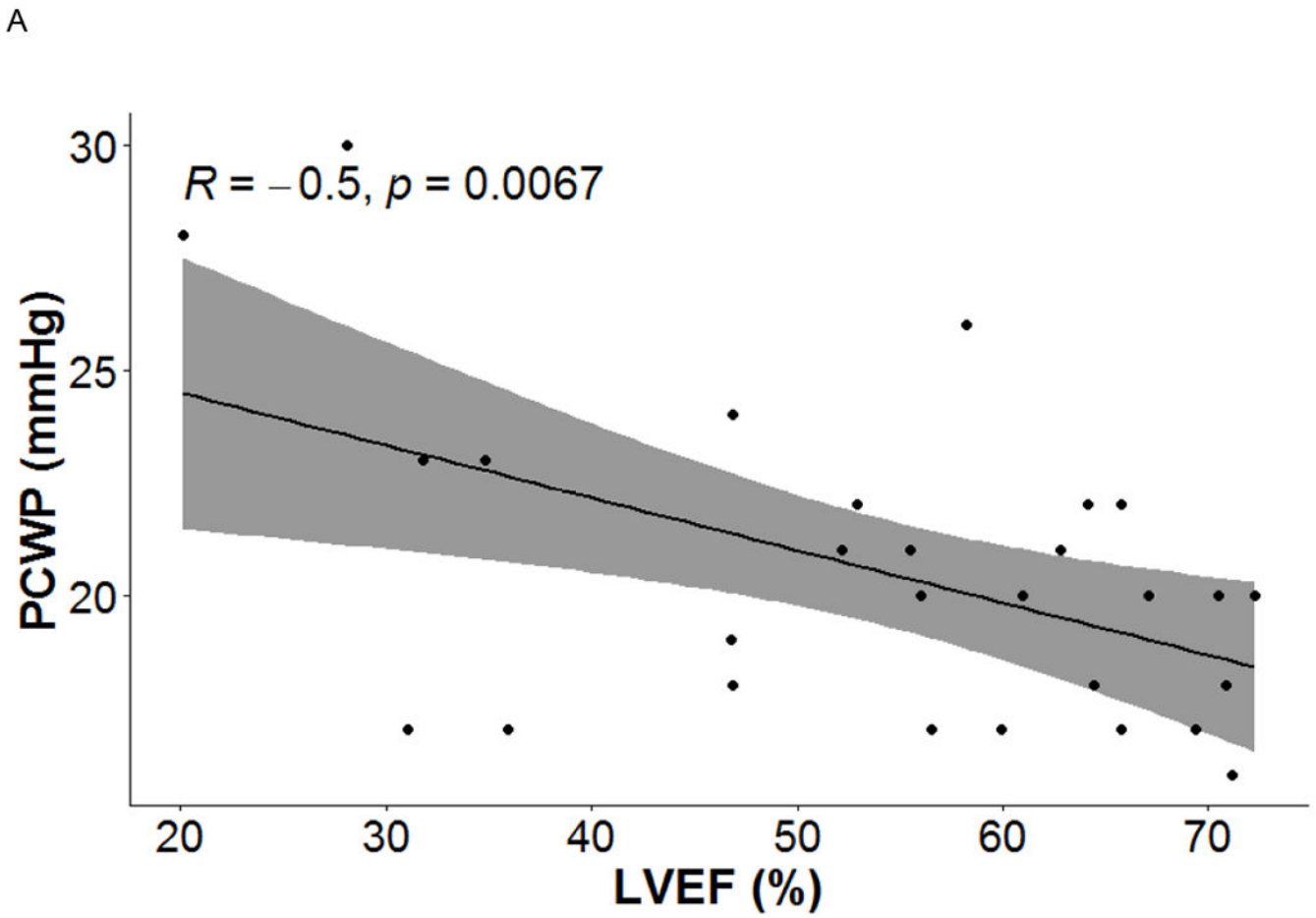

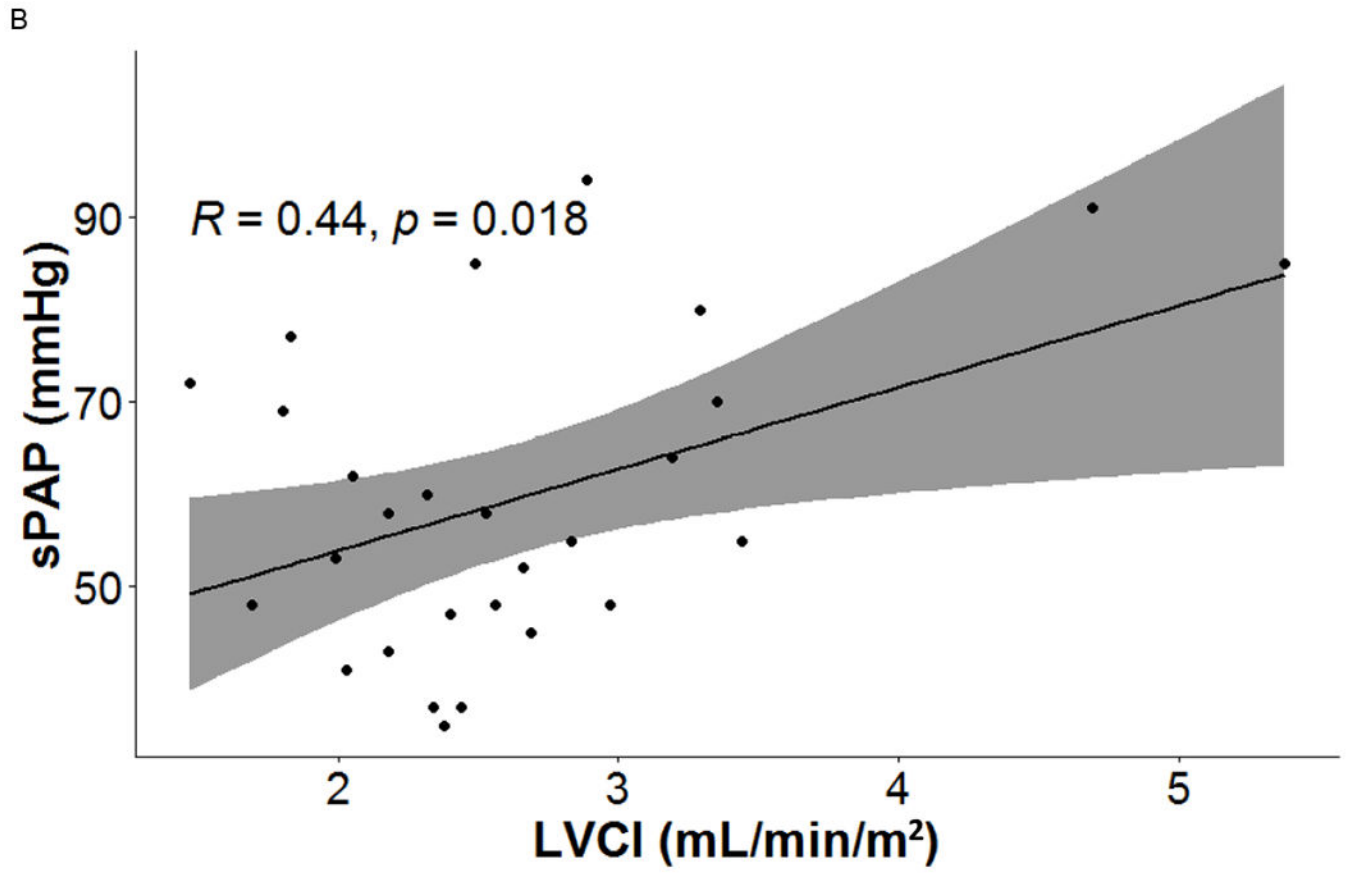

Figure 2.
Cine MRI-derived left heart indices were linearly related with right heart measurements presenting the severity of PH.

Table 1

Demographic, clinical information, RHC results and cine MRI-derived LV/RV functional indices of HFpEF and HFrEF patients

	HFpEF (n = 19)	HFrEF (n = 9)	P values
Age (years old)	59.8 ± 12.7	60.7 ± 16	0.884
Male (%)	6 (26)	5 (56)	0.212
Height (cm)	168 ± 10	168.2 ± 5.8	0.95
Weight (Kg)	94.4 ± 27.6	92 ± 17.4	0.817
BMI	33.2 ± 8.6	32.4 ± 5.2	0.8
PCWP (mmHg)	19.7 ± 2.5	22.1 ± 4.8	0.091
sPAP (mmHg)	60.5 ± 19.1	57.8 ± 11.7	0.701
dPAP (mmHg)	25.7 ± 9.4	26.4 ± 7	0.843
mPAP (mmHg)	37.3 ± 10	38.7 ± 8.2	0.719
PVR (Wood units)	4.2 ± 3.1	3.5 ± 1.4	0.61
Cpc-PH (%)	8 (42)	5 (56)	0.398
LVEF (%)	63 ± 6.4	35.8 ± 9.4	*
LVM (g)	98.8 ± 21.8	125.9 ± 24.2	0.006
LVEDV (mL)	143.5 ± 57.5	193.4 ± 59.1	0.043
LVESV (mL)	54.6 ± 30.2	127.1 ± 48.6	< 0.001
LVSV (mL)	88.9 ± 29.5	66.3 ± 22.5	0.052
LVCO (L/min)	6 ± 2.2	4.4 ± 1.1	0.06
LVCI (L/min/m^2)	2.9 ± 0.9	2.2 ± 0.6	0.033
RVEF(%)	49.4 ± 11.4	40.2 ± 15.2	0.086
RVEDV (mL)	176.3 ± 53	162 ± 37.3	0.474
RVESV (mL)	92.2 ± 43.7	99.6 ± 44.2	0.681
RVSV (mL)	84.1 ± 23.5	62.4 ± 25.2	0.035
RCVO (L/min)	5.6 ± 1.8	4.1 ± 1.3	0.036
RVCI (L/min/m^2)	2.8 ± 0.9	2 ± 0.7	0.041

* No comparison was performed on LVEF because patients were grouped by LVEF.

Table 2

p values of comparing displacement, velocity, strain and strain rates between PH-HFpEF group (n = 19) and PH-HFrEF group (n = 9). PH-HFpEF patients has higher peaks of multiple LV displacement, velocity, strain and strain rate in systolic, early and late diastole than that of PH-HFrEF patients. P values < 0.05 were highlighted.

			HFpEF	**HFrEF**	**P values**
Displacement (cm)	Radial	Systole	1.12 ± 0.27	0.77 ± 0.21	0.002
		Early diastole	0.98 ± 0.41	0.62 ± 0.23	0.022
		Late diastole	0.48 ± 0.2	0.33 ± 0.12	0.051
	Circumferential	Systole	0.36 ± 0.1	0.32 ± 0.12	0.422
		Early diastole	0.24 ± 0.11	0.3 ± 0.1	0.167
		Late diastole	0.26 ± 0.14	0.26 ± 0.1	0.895
Velocity	Radial	Systole	30.7 ± 6	20.4 ±5.3	< 0.001
		Early diastole	27.8 ± 10.1	19.6 ± 2.5	0.025
		Late diastole	13.3 ± 6	9.9 ± 4.9	0.152
	Circumferential	Systole	9.85 ± 3.12	8.49 ± 2.74	0.274
		Early diastole	6.84 ± 2.78	8.41 ± 2.68	0.17
		Late diastole	5.91 ± 3.46	7.47 ± 3.12	0.261
Strain	Radial		33.3 ± 9.1	18.7 ± 7.1	< 0.001
	Circumferential		17.7 ± 3.4	10.9 ± 2.7	< 0.001
Strain rate	Radial	Systole	154.6 ±31.9	83.2 ± 24.3	< 0.001
		Early diastole	178.5 ±72.2	89.6 ± 30.6	0.002
		Late diastole	62.1 ± 34.5	31.1 ± 13.8	0.016
	Circumferential	Systole	91.9 ± 17.4	59.1 ± 16.7	< 0.001
		Early diastole	75.7 ± 28.8	40.2 ± 13.4	0.002
		Late diastole	43.7 ± 19.5	26.2 ± 15.5	0.027

• No diastolic peaks were identified for radial or circumferential strains